Supporting Information

Uniaxial strain controlled ferroelastic domain evolution in $BiFeO_3$

Abdullah Alsubaie[1,2], Pankaj Sharma[1,*], Jin Hong Lee[3,4], Jeong Yong Kim[4], Chan-Ho Yang [4,5], and Jan Seidel[1,*]

[1] School of Materials Science and Engineering, UNSW Sydney, Sydney NSW ~~2032~~, Australia

[2] School of Physics, Taif University, Taif, Kingdom of Saudi Arabia

[3] Unité Mixte de Physique, CNRS, Thales, Université Paris Sud, Université Paris-Saclay, 91767 Palaiseau, France

[4] Department of Physics, KAIST, Yuseong-gu, Daejeon 34141, Republic of Korea

[5] KAIST Institute for the NanoCentury, KAIST, Yuseong-gu, Daejeon 34141, Republic of Korea

*email: pankaj.sharma@unsw.edu.au, jan.seidel@unsw.edu.au

S1: Strain calculation

The strain calculation can be found in our previous published work in references [22, 26] in the main text. For convenience we restate it below.

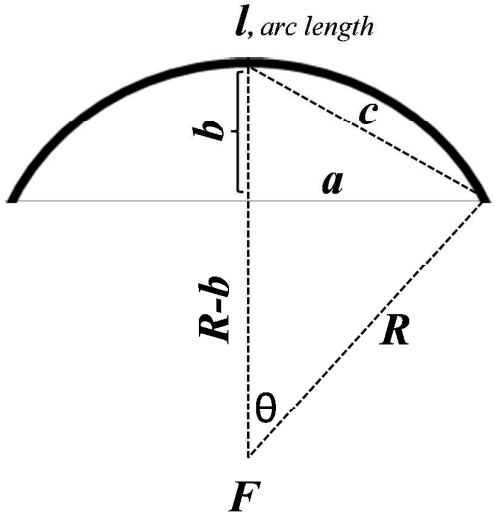

Figure S1 (a): schematic diagram of the bent wafer used for strain calculation.

Strain calculation can be measured using the strain engineering formula:

$$\in = \frac{l-L}{L} \qquad (1)$$

where L is the original length, and l is the length of the sample on application of stress.

In our case, $L = 2a$ with the situation shown in figure S1 (a), the strain formula in equation (1) can be rewritten as:

$$\in = \frac{l-2a}{2a} \qquad (2)$$

Where l is the arc length (final length of the sample), $2a$ is the measured initial length of the sample = 4mm.

$$\text{The arc length, } l = 2R\theta \qquad (3)$$

Where R is the radius of arc (curvature) and θ is the centre angle of the arc.

The radius of curvature R can be written as: [1,2]

$$R = \frac{a^2 + b^2}{2b} \qquad (4)$$

where b is the bending height (height change due to deformation of the center of the sample with respect to the unbent sample). The dashed triangle is selected to obtain the arc angle as:

$$Sin\ \theta = \frac{c}{R} \qquad (5)$$

The length c by Pythagorean Theorem is $\sqrt{a^2 + b^2}$.

The parameters used in the present case are $2a$= 4mm, b is varied at 0.145 and 0.221 mm and the corresponding values of l determined from equations (3-5) are 4.021 and 4.049 mm respectively. Note that $2a$ is the initial measured length of the sample. From equation (*2)*, the obtained values of strain for the 3 cases are: 0 (unbent case), 0.5 and 1.2 %.

In our measurement, b is a variable value due to application of variable mechanical force by pushing at the centre with a screw proceeding upward, by which the pristine wafer was bent. Figure S1 (b) shows the determined curvature of the bent wafer as a function of b. The maximum imposed deflection for our samples was equal to (b) 221 μm corresponding to a curvature of approximately 0.1 $mm^{-1,}$ or tensile strain of 1.2%.

The plot of strain value as a function of the bending height b is shown in figure S1 (c). The obtained 1.2 % tensile strain is the maximum strain that was applied in our measurement with 0.221 mm total deformation at the centre of the sample. The tensile strain values of 0.5% and 1.2% are applied in PFM images [figure 2 in main text].

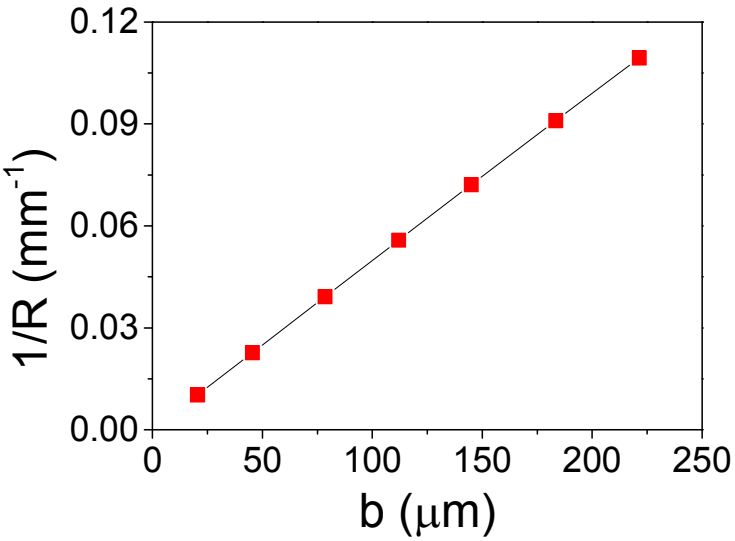

Figure S1 (b): Measured curvature of the bent wafer.

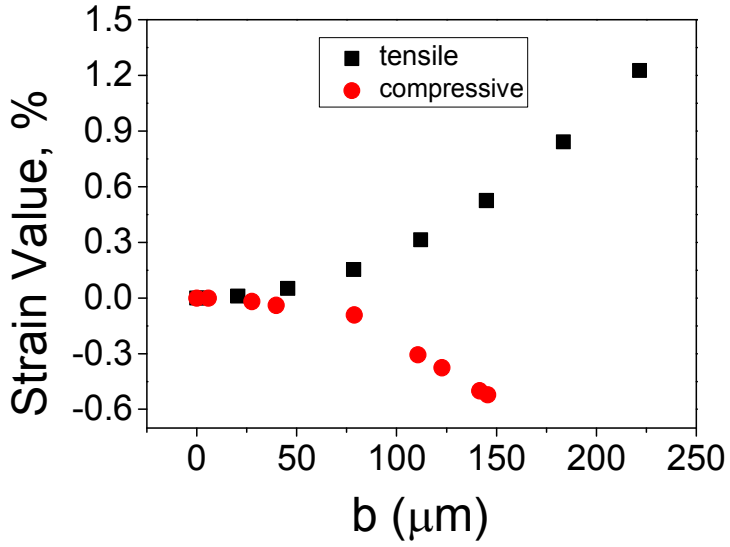

Figure S1 (c): Tensile and Compressive strain as a function of bending height *b*.

S2: Applied mechanical strain measurements performed inside SPM

The strain was applied using the bending stage inside the SPM equipment. The resulting samples were thinned down (to approx. 70 μm) by polishing the backside of the STO substrate and were then glued onto a steel wafer on to which a uniaxial mechanical strain was applied. The dimension of the steel wafer is 3cm×1cm×0.05cm. The <110> direction of the STO substrate was aligned along the long axis of the wafer. Afterwards the wafer was clamped by the bending stage at the two ends. By pushing at the centre with a screw preceding upward the pristine wafer was bent. Figure S2 shows the diagram of the pristine unbent and bent sample/steel wafer. Bending experiments were conducted with a 3-point bending stage such that an external variable uniaxial stress could be applied to the thin film. The bending leads to a visible curvature of the sample and accessible strain values of a few percent without breaking the sample. PFM images were acquired *in-situ* to visualize domain evolution for different applied mechanical strains of a fixed value (i.e., fixed bending) [Figure S2]. More details about the bending stage can be found elsewhere, Ref- [22, 26] in the main text. We note that 1.2% is the maximum strain we applied to the thin film to prevent breaking (as application of strain above 1.2% led to a mechanical breakdown of the sample). Also, given the thickness of the BFO film (60 nm) was several orders of magnitude smaller compared with the 70 micron thick STO layer, the strain in the film can be essentially regarded as homogeneous (i.e., it can be envisioned as "stretching" the film).

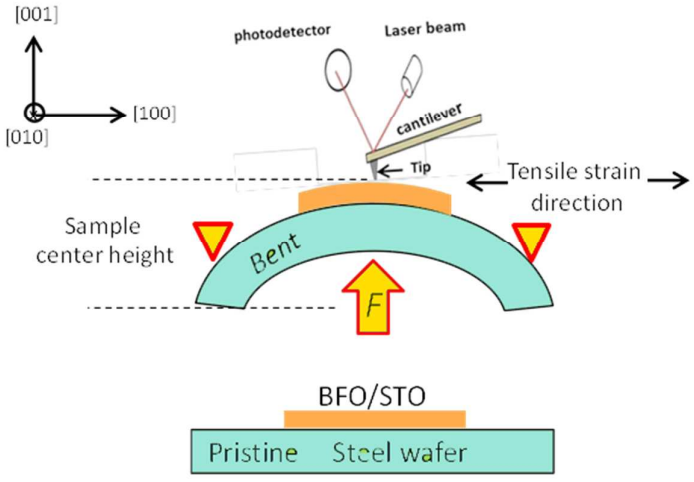

Figure S2: Schematic of the pristine unbent and bent sample/steel wafer. By pushing the steel wafer at the center a uniaxial stress is applied in the BFO thin film.

S3: Mechanism of domain motion under in-situ external stimuli

The applied mechanical stress induces instability between the neighbouring in-plane domains, and the energy barrier for transitioning to a polarization state along the direction of the applied mechanical stress decreases. This is visualized schematically in Figure S3(a). Under applied tensile strain (Fig. S3(a)), the in-plane polarization oriented parallel to the strain direction remains (more or less) unaffected, while the polarization oriented orthogonally decreases in magnitude and eventually realigns (switches) along the direction of applied mechanical strain.

Usually, polarization switching proceeds via both the domain wall motion and nucleation of new domains of opposite polarity.[22] However, in our case (Figure 2 main text), the switching or the domain evolution takes place via domain wall motion only. This is likely due to low activation energy needed for the displacement of an existing domain wall compared to nucleation and growth of new domains (with polarization orthogonal to those of existing domains) within existing domains.

Therefore, the wall front acts as a favourable nucleation site for domains with polarization oriented along the direction of the applied strain (Figure S3(b)). As a result, under an applied mechanical stimulus the domain wall can be visualized to displace from its initial position smoothly unit-cell by unit-cell (Figure S3(b), top left schematic) resulting in polarization switching and evolution of domains. However, random distributions of pinning sites along wall front hinder domain wall propagation at certain locations along the wall. This leads to increasing roughening of the ferroelectric domain wall as shown in the Figure S3(b), bottom left schematic. At positions free of any pinning sites, the domain wall moves with considerable ease under an applied external stimulus, while at others it remains pinned unless higher activation energy is supplied. As a result, domain wall acquires an irregular shape because of random continuous sequence of pinning-depinning transitions along the wall propagating wall front.

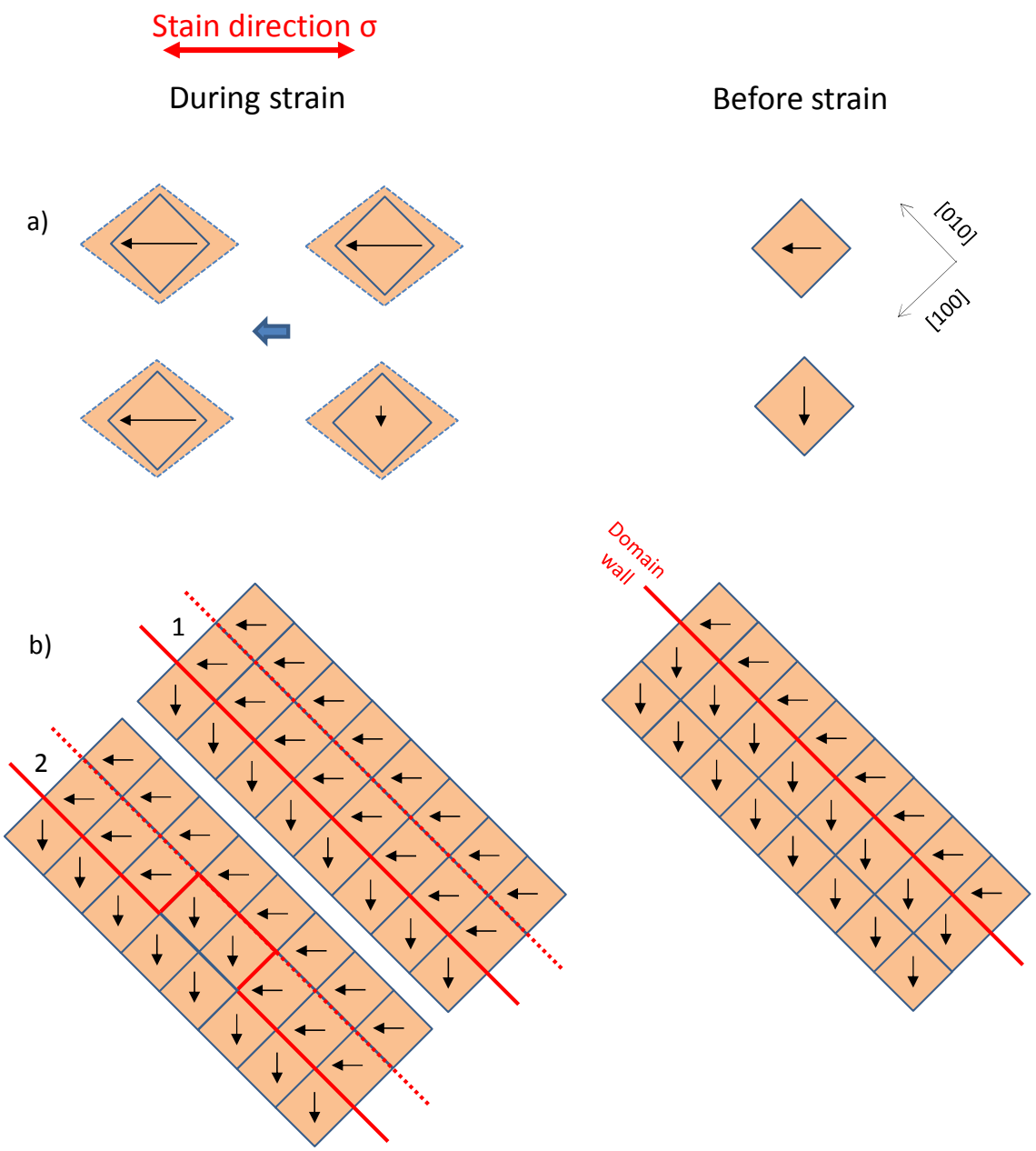

Figure S3: The evolution of polarization (a), and domains (b) during applied mechanical stress. In (a-b), black arrow within the unit cell (top-view) denotes orientation of the in-plane polarization. The schematics in the left column correspond to the state under applied stress, while those in the right column to the pristine state. In (b), solid red-line corresponds to the present location of the wall whereas dotted red-line corresponds to the original position of the wall in the stress-free state.

References:

(1) Gupta, M.; Gupta, A.; Chakravarty, S.; Gupta, R.; Gutberlet, T. Iron self-diffusion in Fe Zr/^{57}Fe Zr Multilayers Measured by Neutron Reflectometry: Effect of Applied Compressive Stress. *Phys. Rev B*. **2006**, 74, 104203.

(2) Chen, J.; De Wolf, I. Study of Damage and Stress Induced by Backgrinding in Si Wafers. *Semicond. Sci. Technology*. **2003**, 18 261-268.